

VILNIUS UNIVERSITY
INSTITUTE OF PHYSICS

Martynas Kinka

DYNAMICS OF POLAR AND FERROELECTRIC MATERIALS CONFINED IN
NANOPOROUS MEDIA STUDIED BY MEANS OF DIELECTRIC SPECTROSCOPY

Summary of doctoral dissertation
Physical sciences, PHYSIC (02 P)

Vilnius, 2009

The study has been performed in 2004–2008 at the Department of Radiophysic, Faculty of Physic, Vilnius University.

Scientific Supervisor:

prof. habil. dr. Jūras Banys (Vilnius University, Physical sciences, Physic – 02 P)

The thesis will be defended at the Scientific Council of Vilnius University, Faculty of Physic:

Chairman

prof. habil. dr. Liudvikas Kimtys (Vilnius University, Physical sciences, Physic – 02 P)

Members:

prof. habil. dr. Arūnas Krotkus (Semiconductor Physic Institute, Physical sciences, Physic – 02 P)

prof. habil. dr. Vytautas Balevičius (Vilnius University, Physical sciences, Physic – 02 P)

habil. dr. Evaldas Tornau (Semiconductor Physic Institute, Physical sciences, Physic – 02 P)

prof. dr. Artūras Jukna (Vilnius Gediminas Technical University, Physical sciences, Physic – 02 P)

Opponents:

prof. habil. dr. Antanas Feliksas Orliukas (Vilnius University, Physical sciences, Physic – 02 P)

prof. habil. dr. Albertas Laurinavičius (Semiconductor Physic Institute, Physical sciences, Physic – 02 P)

The thesis will be presented on September 15, 2009 at the meeting of Doctoral Committee at the Vilnius University, Faculty of Physic.

Address: Saulėtekio av. 9, LT-10222 Vilnius, Lithuania

Summary of the thesis was mailed on August 14, 2009

The thesis is available at the libraries of Vilnius University and Institute of Physic.

VILNIAUS UNIVERSITETAS
FIZIKOS INSTITUTAS

Martynas Kinka

POLINIŲ DARINIŲ IR FEROELEKTRIKŲ, ESANČIŲ NANOPOROSE,
DINAMIKOS TYRIMAS DIELEKTRINĖS SPEKTROSKOPIJOS METODU

Daktaro disertacijos santrauka
Fiziniai mokslai, fizika (02 P)

Vilnius, 2009

Disertacija rengta 2004–2008 metais Vilniaus universitete.

Mokslinis vadovas:

prof. habil. dr. Jūras Banys (Vilniaus universitetas, fiziniai mokslai, fizika – 02)

Disertacija ginama Vilniaus universiteto Fizikos mokslo krypties taryboje:

Pirmininkas

prof. habil. dr. Liudvikas Kimtys (Vilniaus universitetas, fiziniai mokslai, fizika – 02)

Nariai:

prof. habil. dr. Arūnas Krotkus (Puslaidininkų fizikos institutas, fiziniai mokslai, fizika – 02)

prof. habil. dr. Vytautas Balevičius (Vilniaus universitetas, fiziniai mokslai, fizika – 02)

habil. dr. Evaldas Tornau (Puslaidininkų fizikos institutas, fiziniai mokslai, fizika – 02)

prof. dr. Artūras Jukna (Vilniaus Gedimino technikos universitetas, fiziniai mokslai, fizika – 02)

Oponentai:

prof. habil. dr. Antanas Feliksas Orliukas (Vilniaus universitetas, fiziniai mokslai, fizika – 02)

prof. habil. dr. Albertas Laurinavičius (Puslaidininkų fizikos institutas, fiziniai mokslai, fizika – 02)

Disertacija bus ginama viešame Fizikos mokslo krypties tarybos posėdyje 2009 m. rugsėjo mėn. 15 d. Vilniaus universitete, fizikos fakultete.

Adresas: Saulėtekio al. 9, LT-10222 Vilnius, Lietuva

Disertacijos santrauka išsiuntinėta 2009 m. rugpjūčio mėn. 14 d.

Disertaciją galima peržiūrėti Vilniaus universiteto bei Fizikos instituto bibliotekose.

Introduction

The tendency of miniaturization in electronics constantly produces the need of new materials — composites and, of course, new ways for use of well-known ones. Recently much attention in research on ferroelectrics is paid on the size effect—changes of various physical properties when the particle size is reduced to the range of nanometers as well as complete vanishing of ferroelectricity below a certain critical size of the particles. This critical size may amount to a few or some tens of nanometers, and was recently reported to depend on temperature [1]. While these effects are in general predictable by an extended Landau-Ginzburg theory, it is not yet feasible to produce reliable numerical predictions, as we are not dealing with ideal systems but with a complicated interplay of partially delicate and hard-to-control influences, such as sample preparation, free charge layers on surfaces, shape and size distribution, and others. Therefore, it is desirable to enforce the experimental basis of this rather young branch of science, at best with a maximum set of controlled or controllable parameters. One idea is to enclose the ferroelectric sample into matrices of porous materials, in order to start from a system of known geometry. By this, geometry induced influences are reduced and we are able to concentrate on parameters that are better manageable. Such nanostructures in porous matrices have several advantages compared to systems of quasi-isolated ferroelectric particles, viz., the stability of their properties due to confinement, which prevents harmful influence of the atmosphere and at the same time allows the preparation of larger quantities of nanomaterials (at least several cubic centimeters). The latter is hardly achievable by conventional methods of nanostructure preparation, such as nanolithography and molecular beam epitaxy.

One of the main problems for such investigations was the lack of well-characterized materials having a simple pore geometry. This often made interpretation of experimental results quite difficult and even contraversary [2]. Novel MCM – 41 materials are very suitable and promising media for such investigations because of their unique structural and chemical properties. This class of silica tube-like materials features extremely large specific surface areas exceeding $1000 \text{ m}^2 \text{ g}^{-1}$ and possess uniformly sized mesopores whose diameter can be controlled between 1.5 and 8 nm by the synthesis conditions chosen and template used [3,4]. The silicon can be partially substituted by various metal ions [5] in order to modify the chemical (hydrophilic) properties of the

inner surface of the molecular sieve materials. the relatively large pore size allows the fixation of catalytically active complexes [5, 6] and metal clusters [5, 7] at the surface of the mesopores. Thus, MCM-41 materials have especially attracted interest in adsorptive and catalytic applications involving large molecules [5]. Other promising applications are the use of MCM-41 materials as hosts for semiconducting [8–11] and ferroelectric [12] nanomaterials as well as for the study of confined liquids [13–17] and polymers [17, 18]. Many of the envisaged applications involve aqueous phases at one or the other step. Therefore information about the structure, dynamics, and freezing phenomena of water confined in the mesopores is of uttermost importance to control and optimize catalytic activity or pore fillings by guest molecules.

It should be emphasized that nanostructures within porous matrices can be studied by the same experimental techniques which are used for bulk ferroelectric substances. Dielectric spectroscopy among them is one of the best techniques to study the relaxation dynamics of such systems due to its very broad frequency range and almost unlimited temperature usage region. If ferroelectric materials are imbedded into pores, however, not only the influence of interactions between the nanoparticles but also of those with the inner surface of the porous matrices has to be understood.

The aim and tasks of this dissertation

The aim of this dissertation is to investigate the dynamics of water, methanol and various ferroelectrics, confined in different nanoporous materials, by means of dielectric spectroscopy in wide frequency and temperature ranges.

Main tasks:

- 1) Measure dielectric responses of water adsorbed in various mesoporous materials with different structure and pore size to investigate peculiarities of melting-freezing dynamics. Ascertain the influence of pore size, structure and chemical composition of the hosting matrix on the dynamics of adsorbed molecules.
- 2) Measure dielectric responses of methanol adsorbed in different MCM-41 mesoporous molecular sieves to investigate peculiarities of melting-freezing dynamics. Ascertain the influence of partial substitution of Si atoms with Al in

chemical composition of MCM-41 materials on the dynamics of adsorbed molecules.

- 3) Investigate dielectric properties in the dispersion region of betaine phosphite, barium titanate and sodium nitrite confined in different MCM-41 molecular sieves and porous glasses.

The novelty of obtained results

- 1) Dielectric responses of all composite systems under investigation here were systematically measured for the first time in such wide frequency and temperature ranges.
- 2) Distributions of relaxation times of confined water and methanol molecules that are strongly interacting with the hosting matrix were calculated for the first time and temperature dependencies of most probable relaxation times were obtained.
- 3) Temperature dependencies of the relaxation time of betaine phosphite confined in MCM-41 molecular sieves with different pore sizes were obtained and ferroelectric phase transition temperatures were determined for the first time.
- 4) Temperature dependencies of the relaxation time of sodium nitrite confined in porous glass with 7 nm and 20 nm pore sizes were obtained.

Statements presented for defence

- 1) Very broad distributions of relaxation times are characteristic for confined water and methanol molecules that are strongly interacting with the hosting matrix, which are caused by the formation of highly disordered hydrogen bonded network at low temperatures ($T < 220$ K). Temperature evolution of most probable relaxation times depends on the pore size and chemical composition of the hosting matrix.
- 2) Ferroelectric phase transition temperatures of betaine phosphite confined in MCM-41 molecular sieves are lower than those for bulk crystals. Confinement also changes the dynamics of betaine phosphite in the vicinity of the phase transition temperature.
- 3) No ferroelectric phase transitions were observed for barium titanate confined in MCM-41 molecular sieves. Permittivity maximums at 305 K and 315 K in

dielectric responses are caused by adsorbed water and not by a ferroelectric phase transition (as suggested earlier).

- 4) Dielectric response of sodium nitrite confined in porous glasses is dominated by a giant increase of permittivity at low frequencies, which is caused by formation of a premelted phase. Relaxational soft mode temperature behaviour is also different from classical ferroelectrics. Only change in the activation energy can be identified as phase transition.

Outline of the dissertation

The dissertation consists of 4 chapters followed by conclusions as well as a references section. Introduction, main goals of the investigations, general problems to be solved, scientific novelty, practical importance and main statements to be defended are presented in **Chapter 1 (Introduction)**.

Chapter 2 is devoted to overview of the main up to date results obtained in the field of investigations of confined materials.

At first, a short introduction about history of synthesis, classification and main properties of porous materials, usually used as a hosting matrix, is given. Later a greater attention is paid only to those porous materials which were used in this work for investigations. Synthesis procedures, structure, pore geometry and common physical properties are listed for porous glasses, MCM-41 molecular sieves and metal-organic frameworks.

The next section gives a literature overview on investigations of freezing-melting dynamics of confined liquids. The fundamental interest in this area is the desire to understand the new physics that occurs due to finite-size effects, surface forces and reduced dimensionality. The importance of size reduction, fluid-fluid and fluid-wall interactions in these systems must be emphasized, which usually drastically change most of the properties of confined liquids compared to the bulk. Confinement can lower or increase freezing-melting temperature and sometimes even induce the appearance of new surface driven and confinement driven phases of adsorbed material. The nature of these phases, their structure and properties (e.g. diffusion rates, shear properties etc.) and their relation to the surface forces, pore dimensions and pore morphology and topology are of

considerable interest, and are at present not well understood. Both theoretical and experimental works in this field are beset with significant difficulties, cause numerous complications (metastable states, surface heterogeneity, pore connectivity) can occur in experimental systems.

The last section is devoted to the overview of a recent progress in investigations of nanosized ferroelectrics. In recent years size effects on critical temperatures of ferroelectric materials $T_c(D)$ have been extensively investigated theoretically and experimentally due to their scientific and industrial importance (T_c signifies the critical temperature and D denotes the diameter of nanoparticles and nanowires or the thickness of thin films). It is found that $T_c(D)$ progressively reduces with decreasing D . For free nanoparticles or nanowires, the most important influence on $T_c(D)$ seems to be the size. If the interactions between for example the particles and the substrates or a holding matrix are weak compared to the inner interaction of the ferroelectric particle, the size effect is also the dominant factor affecting the $T_c(D)$ suppression. Otherwise, the substrate or hosting effect becomes evident. Surface and interface contributions on $T_c(D)$ are complicated cause usually the chemical interaction at the interface cannot be quantitatively determined. The majority of experimental results have been obtained for thin films or granular materials. There is one new method of preparation of such nano ferroelectrics becoming more and more popular - an intrusion of materials into artificial or natural porous matrices. Namely results of investigation of such new nanocomposites are presented in this dissertation work.

Chapter 3 covers the description of experimental methods and instrumentation used during measurements.

At low frequencies (20 Hz – 1 MHz), the dielectric permittivity data has been collected by measuring the capacitance and tangent of loss of samples using LC meter. In high frequency region (1 MHz – 3 GHz), the dielectric permittivity of specimens have been calculated from the measured complex reflection coefficient using vector network analyzer. The disc-shaped samples were placed in the vertical coaxial line between the inner conductor and short end, which were freshly polished for each measurement for better electrical contact (due to the porosity of samples it was not possible to cover them

with silver or gold electrodes). Measurements have been performed on cooling and heating at a rate of about 0.5 K min^{-1} .

Personally obtained results of investigation of properties of confined materials using dielectric spectroscopy are presented in **Chapter 4**. This chapter is further divided into five sections, each corresponding to a different confined material.

Section 4.1 is devoted to water properties inside MCM-41 (with different pore sizes $d = 2 \text{ nm}$, $2,5 \text{ nm}$ and $3,7 \text{ nm}$) and Al MCM-41 ($d = 3,8 \text{ nm}$, with three different Al ratios in pore framework, namely $\text{Si/Al} = 64$, 16 and 2) molecular sieves, porous glasses ($d = 7 \text{ nm}$, disordered pores) and Co-metalorganic frameworks ($d = 0,44 \text{ nm}$).

Studies of water confined in other silica based pores showed different structural and dynamical properties of confined water compared to the bulk. Always a depression of the freezing point was observed along with the freezing-melting hysteresis [13]. The shift of the freezing temperature shows good agreement with the Gibbs-Thomson equation for pores larger than 5 nm and quite big deviations were observed for smaller pores [19]. NMR and X-ray diffraction studies revealed several types of water inside pores. “Bound” water – few disordered water molecule layers near the pore walls with a structure that is different from that of the bulk ice and free liquid, relatively free water in the center of the mesopores and intermediate layer between these two [20]. It was found, that water in the centers of mesopores freezes rather to a cubic ice I_c instead of an ordinary hexagonal phase I_h [15]. Also this phenomenon is very dependable on the pore size. It was found that the confined fluid freezes into a single crystalline structure for average pore diameters greater than 20σ , where σ is the diameter of the fluid molecule. For average pore sizes between 20 and 15σ , part of the confined fluid freezes into a frustrated crystal structure with the rest forming an amorphous region. For pore sizes smaller than 15σ , even the partial crystallization did not occur [13].

Obtained dielectric response of water confined in MCM-41, Al MCM-41, porous glasses and metalorganic frameworks shows a rich variety of different water phases with characteristic dynamics. Figure 1 illustrates the temperature dependence of the real and imaginary parts of dielectric permittivity between 100 K and 400 K of adsorbed water in the pure siliceous MCM-41 sample ($d = 3,7 \text{ nm}$) at different frequencies, which is also

characteristic for all other investigated matrixes. There are three dispersion regions of the adsorbed water molecules (Figure 1): (1) at low temperatures between 120 K and 220 K, which is shown in the insert of Figure 1, (2) in the range between 220 K and 400 K and (3) in the temperature range between 280 K and 340 K. We must mark, that no freezing-melting hysteresis was observed for the (1) temperature range. Trying to remove adsorbed water molecules the sample was heated up and kept at $T > 400$ K for two hours. Then, the temperature dependence of the real and imaginary parts of dielectric permittivity of the sample was measured again on a cooling cycle down to 150 K. The obtained results showed that (2) and (3) dispersion regions have disappeared, confirming that relatively “free” water molecules, which were confined in the middle of the pores, almost completely evaporated after the thermal treatment and that (1) dispersion region is caused by more strongly bound water molecules probably in an interfacial layer on the inner surface of the mesopores.

Obtained low temperature frequency dependences of complex dielectric permittivity are much broader than as expected for a Debye-type dispersion of 1.14 decades. Such behaviour of ϵ^* does not allow a reliable estimation of the relaxation time using conventional relaxation models or empirical equations. Therefore, direct calculations of the relaxation time distribution function $g(\tau)$ from the frequency dependence of the complex dielectric permittivity at fixed temperatures according to superposition of Debye-like processes (Eq. 1) were made with the help of original program [21]:

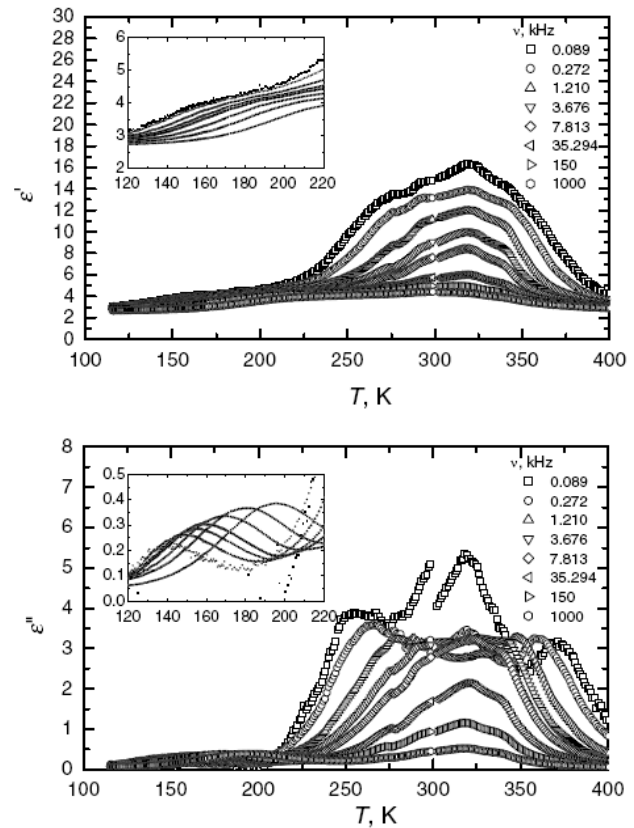
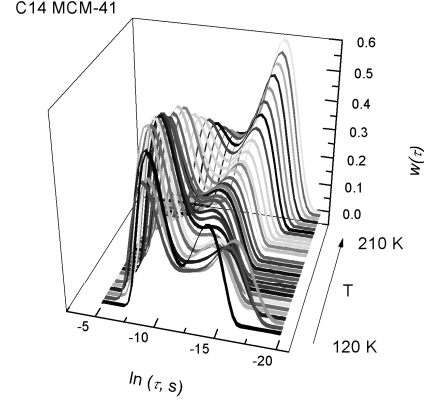


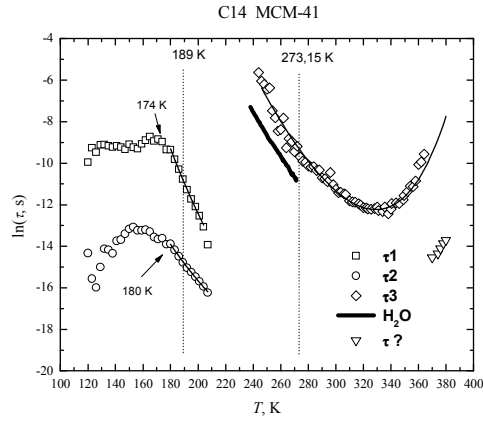
Figure 1. Temperature dependences of the real and imaginary parts of dielectric permittivity of water adsorbed in MCM-41 molecular sieves with 3.7 nm pores.

$$\varepsilon'(\nu) = \varepsilon_{\infty} + \int_0^{\infty} \frac{g(\tau)}{1 + (2\pi\nu\tau)^2} d(\ln \tau) \quad \varepsilon''(\nu) = \int_0^{\infty} \frac{2\pi\nu\tau g(\tau)}{1 + (2\pi\nu\tau)^2} d(\ln \tau) \quad (1)$$

Very broad distributions of the relaxation times were obtained. Strong interaction of water molecules with the pore surface disturbs network of hydrogen bonds and leads to the broadening of the distribution of the relaxation times and increase in the mobility of individual molecules compared with the bulk ice. An example of obtained distributions of relaxation times, which is typical for all samples with water except MOF, is shown in Figure 2a. Two maxima corresponding to two most probable relaxation processes can be distinguished. At low temperatures a slower process is dominating the spectra. With increasing temperature a second (faster) process becomes stronger and finally suppresses the first one. Figure 2b shows typical temperature dependencies of most probable relaxation times τ_1 and τ_2 , corresponding to these two maxima. At low temperatures both relaxation times are almost constant. After certain temperatures they start to decrease more rapidly and their temperature dependencies follow Arrhenius law:



a



b

Figure 2. a) Distributions of relaxation times of adsorbed water molecules at low temperatures. b) temperature dependencies of most probable relaxation times (τ_1 and τ_2) obtained from the calculated distributions of the relaxation time and „saddle like” temperature dependencies of relaxation times (τ_3 and $\tau_?$) obtained in the higher temperature dispersion region compared with the relaxation time of bulk ice (H_2O).

probable relaxation times τ_1 and

τ_2 , corresponding to these two maxima. At low temperatures both relaxation times are almost constant. After certain temperatures they start to decrease more rapidly and their temperature dependencies follow Arrhenius law:

$$\tau = \tau_0 \exp\left(\frac{E}{kT}\right). \quad (2)$$

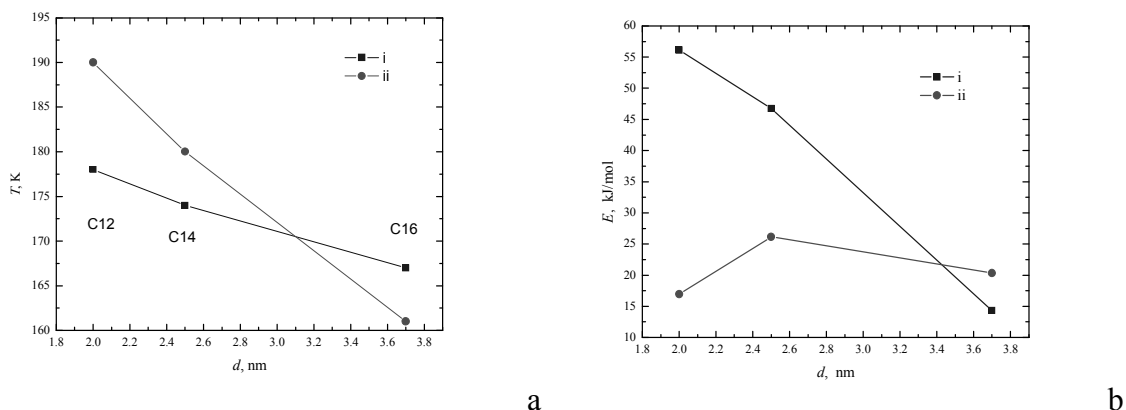


Figure 3. Dependencies of sudden change point temperatures (a) and obtained Arrhenius activation energies (b) on the pore size of MCM-41 molecular sieves for slower (i) and faster (ii) relaxation processes.

This sudden change temperature is different for both processes and is dependent on the pore size of a hosting matrix. Figure 3a shows that it decreases more rapidly for τ_2 with increasing pore size. These results suggest that the slower relaxation process is caused by water molecules that are very close to the pore walls and are strongly confined. This was also confirmed by obtained activation energies from Arrhenius law (Figure 3b). Activation energy for the first process considerably decreases, while for the faster one remains almost constant. All obtained activation energies are smaller than that of a bulk ice (60 kJ/mol).

Incorporation of Al into the framework of MCM-41 molecular sieves

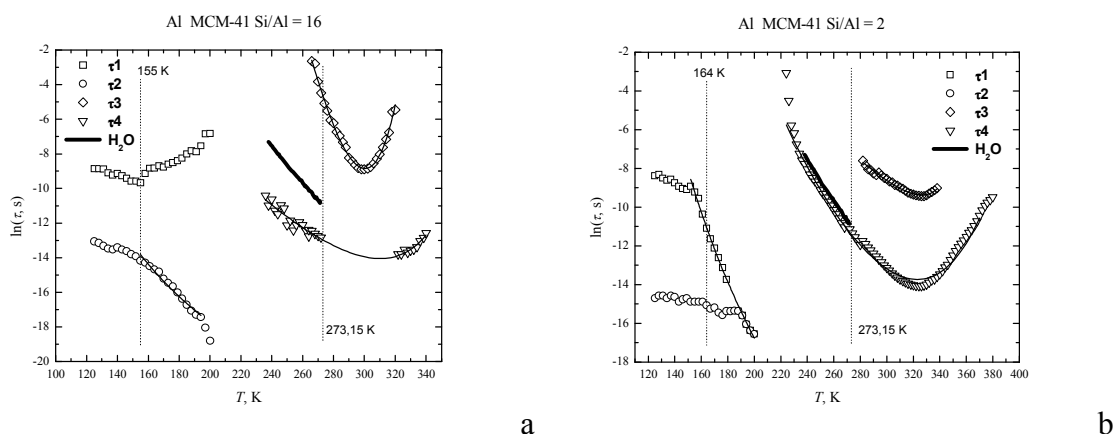


Figure 4. Temperature dependencies of most probable relaxation times (τ_1 and τ_2) obtained from the calculated distributions of the relaxation time and „saddle like” temperature dependencies of relaxation times (τ_3 and τ_4) obtained in the higher temperature dispersion

considerably changes dynamics of adsorbed water molecules. Still two maxima were observed in calculated distributions of the relaxation times, but their temperature

evolution is different. In samples with smaller aluminum amount (Si/Al = 64, 16) no shortening of τ_1 was observed (Figure 4a). Instead it even grows a little bit – a great portion of adsorbed molecules in the interfacial layer stays “immobilized” in the vicinity of Al “defects”. This behavior changes again when Si/Al ratio reaches 2. Both most probable relaxation times start decreasing at certain temperatures, and their temperature dependencies follow Arrhenius law with the same parameters (Figure 4b). Similar τ_1 and τ_2 temperature dependencies were observed also for water confined in porous glass with 7 nm disordered pores.

The second dispersion region, located at higher temperatures, was also observed in all investigated samples. It is caused by two overlapping processes: relaxation of “relatively free” water and conductivity at low frequencies. At first the maximum position of dielectric losses shifts to higher frequencies with temperature, as expected. After reaching a certain value, it decreases with a further increase of temperature. The temperature dependence of the relaxation time of water molecules, obtained from Havriliak – Negami fits including conductivity term, has a “saddle like” shape (Figures 2b and 4). Similar behavior of τ recently was observed for water inside porous glasses [13] and Faujasite-type molecular sieves [22]. According to these authors, this relaxation process is thought to be a kinetic transition due to water molecule reorientation in the vicinity of a defect. Sliwinska,-Bartkowiak and co. workers developed a model based on the idea of Macedo and Litovitz to describe this relaxation process [13]. The main idea is that relaxation is influenced by two simultaneous events: (a) the molecule must have enough energy to break away from it’s neighbors and change its orientation, and (b) there must be a site with a defect in the vicinity of the moving molecule with sufficient local free volume for a reorientation. Then the temperature dependence of the relaxation time can be written as follows:

$$\tau = \tau_0 \exp\left\{\frac{H_a}{kT} + C \exp\left(-\frac{H_d}{kT}\right)\right\}, \quad (3)$$

where H_a is the height of the potential barrier between equilibrium positions, H_d is the energy of the defect formation and $C \sim 1/\eta$ (constant η is the maximum possible defect concentration).

All obtained temperature dependencies of relaxation time in this high temperature dispersion region were fitted using Eq. (3). Calculated parameter values are in good agreement with other's results of investigation of water adsorbed in different porous materials, posted in literature. Nevertheless it should be emphasized, that no direct correlation between these values and pore size or chemical structure of a hosting matrix was found and the dynamics of water molecules at higher temperatures is more dependent on the amount of adsorbed water.

After investigation of water dynamics in metal-organic frameworks with the smallest pores ($d = 0.44$ nm) some interesting results were obtained with several specific features. First of all only one maximum was observed in calculated distributions of relaxation times (Figure 5a). These distributions are much narrower than in previous

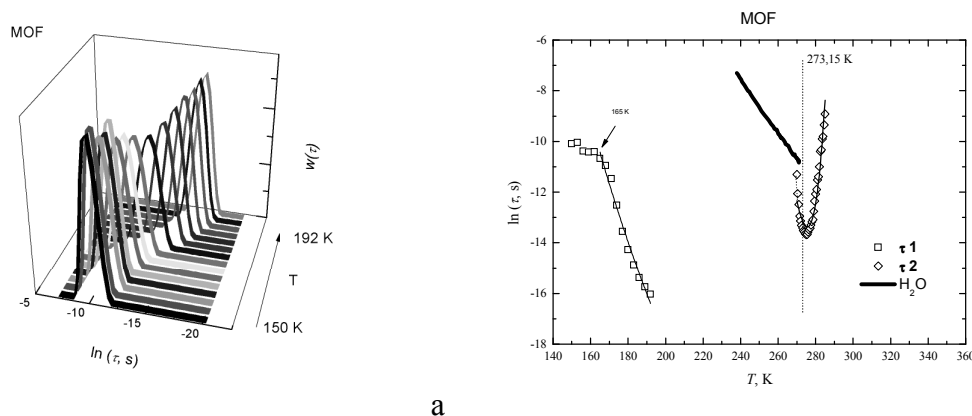


Figure 5. a) Distributions of relaxation times of water molecules adsorbed in MOF at low temperatures. b) temperature dependence of the most probable relaxation time (τ_1) obtained from the calculated distributions of relaxation times and a „saddle like” temperature dependence of the relaxation time (τ_2) obtained in the higher temperature dispersion region compared with the relaxation time of bulk ice (H_2O).

cases mentioned before. The temperature dependence of the most probable relaxation time also experiences a sudden change and afterwards follows Arrhenius law (Figure 5b) with increasing temperature. These differences could be explained by the fact, that the pore volume of MOF is so small, that all adsorbed water molecules almost evenly “feel” the influence of a hosting matrix. In the high temperature dispersion region a saddle like temperature dependence of the relaxation time was obtained, but it is much narrower than in MCM-41 molecular sieves or porous glasses (Figure 5b).

Section 4.2 is devoted to methanol properties inside pure Si MCM-41 ($d = 3,7$) and Al MCM-41 ($d = 3,8$ nm, with two different Al ratios in pore framework, namely Si/Al = 64, 16).

Alcohols are also strongly hydrogen-bonded organic liquids. Methanol being the simplest one is of fundamental interest and a test system for studying the influence of H bonds and fluid–substrate interaction on the properties of confined fluids. Its structural properties have been extensively studied in bulk conditions by neutron scattering [23, 24], x rays [25] and molecular simulation [26, 27]. Phase transitions of methanol confined in regular cylindrical pores of MCM-41 and SBA-15 silicates have been investigated by x-ray diffraction [28]. The freezing/melting behavior depends markedly upon the pore size, with different degrees of hysteresis and metastability. Within the pores of diameter lower than 7.8 nm, crystallization never occurs and the confined methanol ultimately vitrifies at about 100 K close to the value of the bulk glass transition temperature.

The obtained temperature dependencies of the real and imaginary parts of dielectric permittivity of pure siliceous MCM-41 sample with methanol (MEOH) at different frequencies upon heating from 100 K to 400 K are shown in Figure 6. Again dielectric response differs significantly from that of a bulk methanol and two dispersion regions (low and high temperature) of characteristic shape can be distinguished.

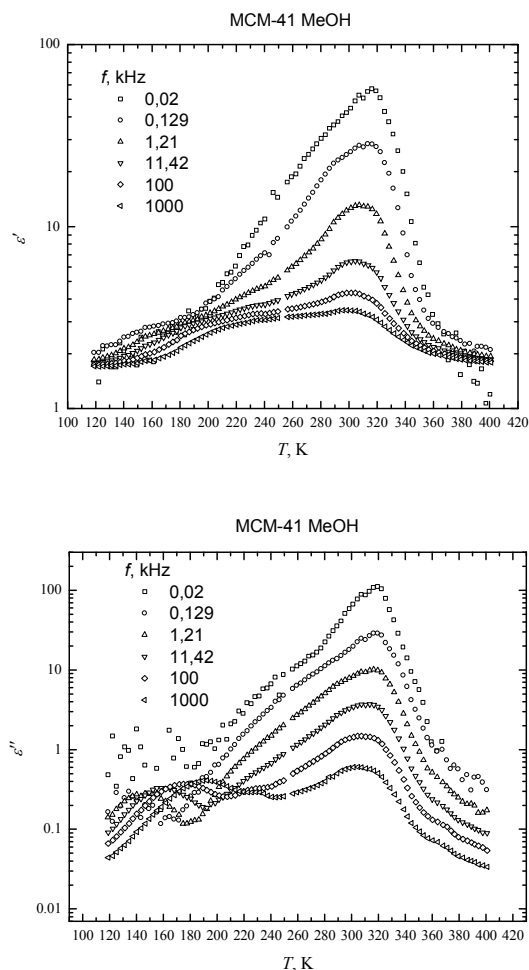


Figure 6. Temperature dependencies of the real and imaginary parts of dielectric permittivity of MeOH confined in MCM-41 material within 3.7 nm pores

Temperature dependences of the dielectric permittivity of other two samples with Si/Al 16 and 64 look very similar.

At low temperatures, like in water case, very broad distributions of relaxation

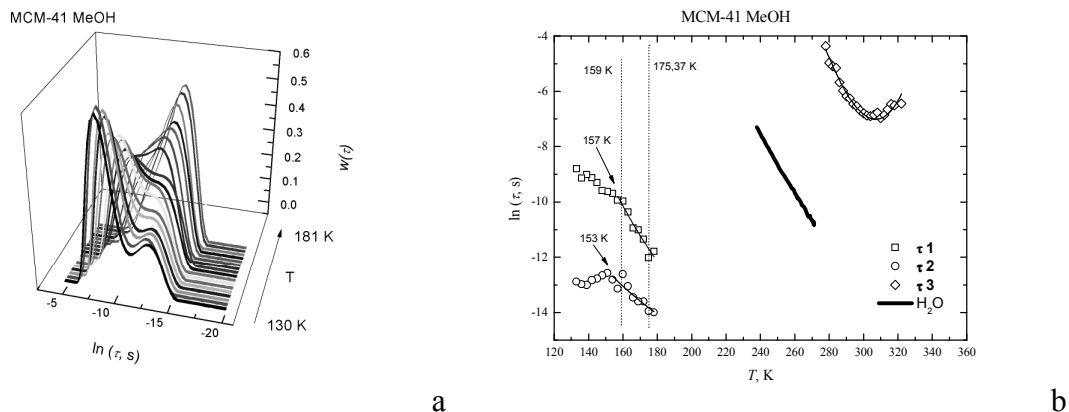


Figure 7. a) Distributions of relaxation times of adsorbed methanol molecules at low temperatures. b) temperature dependences of most probable relaxation times (τ_1 and τ_2) obtained from the calculated distributions of the relaxation time and „saddle like” temperature dependence of the relaxation time (τ_3) obtained in the higher temperature dispersion region compared with the relaxation time of bulk ice (H_2O).

times with two maxima were obtained (Figure 7a). Temperature behavior of the most probable relaxation times is also quite similar (Figure 7b). Obtained sudden change temperatures correlate very well with methanol melting temperatures defined by x-ray diffraction experiments in SBA-15 molecular sieves [28] and activation energies from fits by Arrhenius law are similar to those calculated theoretically [29]. In the high temperature dispersion region saddle like temperature dependences of the relaxation time were obtained again, but they are shifted to lower frequencies compared with water. The increase of Al amount in the framework of MCM-41 molecular sieves markedly affects only the activation energy of the slower process at low temperatures, once more confirming that it is caused by the interfacial adsorbed molecules.

These aforementioned results of investigation of confined methanol support ideas expressed in previous section that hydrogen bonding and fluid – wall interactions play a key role in the dynamics of confined water.

Dielectric properties of betaine phosphite confined in MCM-41 molecular sieves ($d = 2$ nm, 2,5 nm and 3,7 nm) are presented in **Section 4.3**.

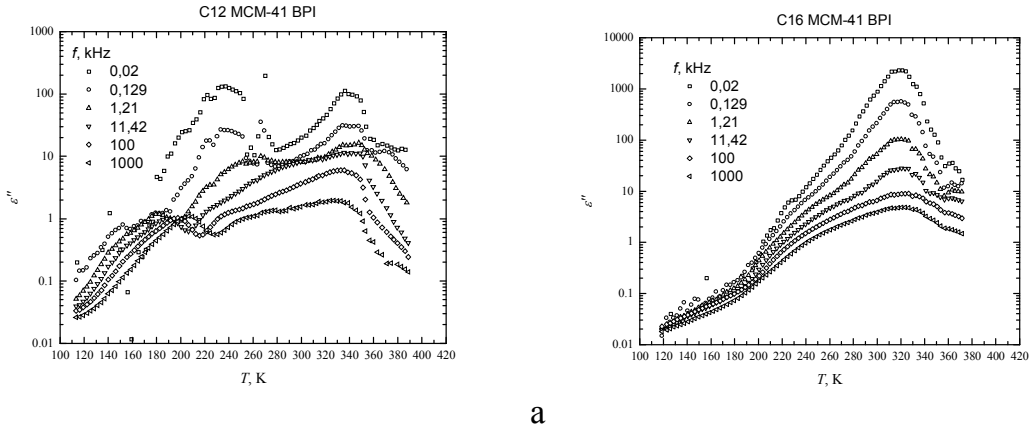


Figure 8. Temperature dependencies of the imaginary part of dielectric permittivity of betaine phosphite containing MCM-41 molecular sieves with 2 nm (a) and 3.7 nm (b) pores.

Betaine phosphite ($(\text{CH}_3)_3\text{NCH}_2\text{COOH}_3\text{PO}_3$) are molecular crystals consisting of the amino acid betaine, as the organic, and phosphorous acids as the inorganic component. The inorganic components (PO_3 groups) are linked by hydrogen bonds to form quasi-one-dimensional chains. The structure of BPI was investigated using x-ray and elastic neutron scattering experiments [30]. It was found that BPI at room temperature is monoclinic (space group $P2_1/c$). BPI crystal also shows two phase transitions on cooling: from paraelectric to antiferrodistorsive phase at 355 K and to the ferroelectric phase at 220 K [31].

Dielectric investigation of the MCM-41 molecular sieve material with ferroelectric betaine phosphite showed complicated dielectric spectra mainly caused by water, but also the influence of BPI was observed. The dielectric spectra of betaine phosphite

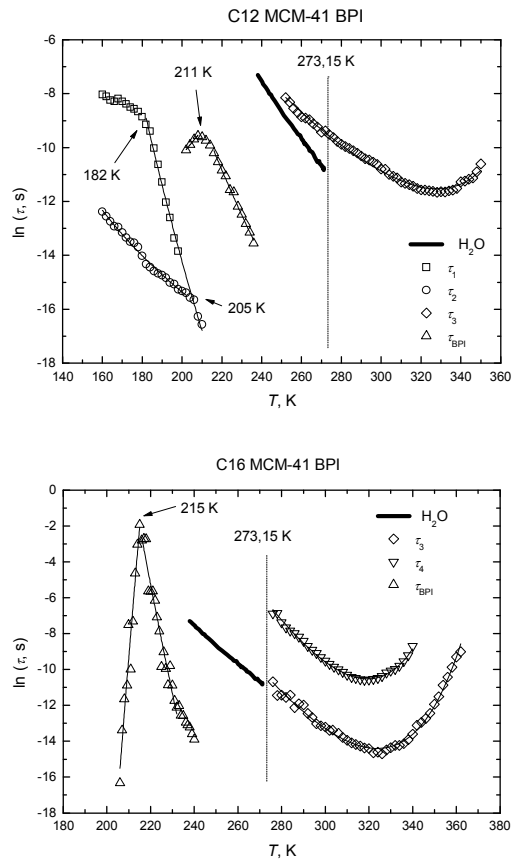


Figure 9. Temperature dependencies of obtained relaxation times of confined water (τ_1 , τ_2 , τ_3) and betaine phosphite (τ_{BPI}).

confined in these molecular sieves was compared with the results obtained from the investigation of pure MCM-41 materials containing water. No big changes were found for the material with the smallest pores, while dielectric response of MCM-41 materials with pores of 2.5 nm and 3.7 nm containing BPI differs significantly from that of the empty ones confirming successful incorporation of ferroelectric material into the porous matrix (Figure 8). Also it must be marked that dielectric response of investigated materials is still strongly influenced by water molecules that were adsorbed during the sample preparation procedure. Saddle like temperature dependencies of the relaxation time of adsorbed water molecules in the high temperature dispersion region were found in all samples (Figure 9). The low temperature dispersion region with characteristic dynamics of strongly confined water was observed only in MCM-41 sample with the smallest pores. Despite the dominating influence of water it is still possible to distinguish relaxation process caused by betaine phosphite molecules inside the pores in all investigated materials. Temperature dependencies of obtained relaxation time are presented in Figure 9. From their maximums ferroelectric phase transition temperatures of confined BPI were determined, which are several degrees lower than that of a bulk betaine phosphite crystal.

Section 4.4 presents dielectric properties of barium titanate confined in Na form and H form MCM-41 molecular sieves ($d = 3,8$ nm).

BaTiO_3 is a typical ferroelectric material for optoelectronic devices with a perovskite structure. On cooling it undergoes three displacive ferroelectric transitions of the first type at 393 K, 278 K and 183 K. Dielectric properties of BaTiO_3 confined in MCM-41 molecular sieves with 3 nm and 4.2 nm pores were investigated by S. Kohiki [12] and E. Bierwirth [32], but only at 100 kHz frequency and temperatures higher than 290 K. In both cases dielectric response showed peak at 305 K - 315 K temperatures which was assigned to be of ferroelectric origin and the significant lowering of ferroelectric transition temperature was concluded.

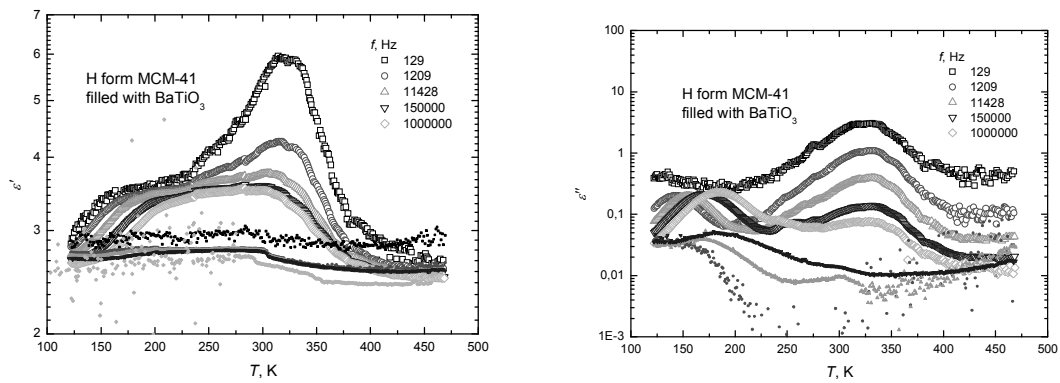


Figure 10. Temperature dependencies of the real and imaginary parts of dielectric permittivity of H-form MCM-41 filled with BaTiO₃ (small symbols – after thermal treatment).

Measured dielectric values of barium titanate confined in Na form and H form MCM-41 molecular sieves are much smaller than those of the bulk BaTiO₃ and only slightly differ from those of the empty carrier material containing water (Figure 10). Also maximums of dielectric permittivity above room temperature were found, which

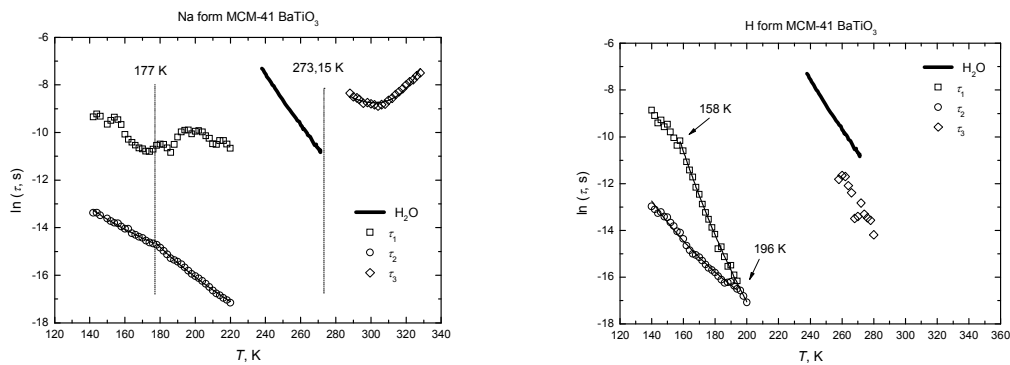


Figure 11. Temperature dependencies of most probable relaxation times (τ_1 and τ_2) obtained from the calculated distributions of the relaxation time and „saddle like” temperature dependence of the relaxation time (τ_3) obtained in the higher temperature dispersion region for water confined in BaTiO₃ containing MCM-41 materials compared with the relaxation time of bulk ice (H₂O).

were reported by S. Kohiki et al. [12] and E. Bierwirth [32]. Nevertheless, a detailed analysis of dielectric spectra in all temperature range showed that these dielectric anomalies are caused by adsorbed water, as characteristic temperature dependencies of relaxation time were obtained (Figure 11). Their temperature evolution and activation energies are slightly affected by BaTiO₃ present inside pores. Also at high temperatures the gradual increase of dielectric permittivity is observed for all frequencies, which was not found for the pure MCM-41. This is one more indication that Barium titanate

molecules are in the pores, but the size of synthesized particles is smaller than the critical size. Therefore, no ferroelectric phase transition was observed for both samples.

Section 4.5 is devoted to dielectric properties of sodium nitrite confined in porous glass with 7 nm and 20 nm pores.

Bulk sodium nitrite is a well known order-disorder type ferroelectric material and it undergoes the first order phase transition at $T_C \approx 437$ K. The temperature evolution of the structure of NaNO₂ nanocomposite ferroelectric material in a porous glass with 7 nm pores was studied by neutron diffraction in temperature region from room temperature up to the melting [33,34], *i.e.* in the ferro- and paraelectric phases. It was demonstrated that in the ferroelectric phase the structure is consistent with the structure of the bulk, but above the ferroelectric phase transition (and up to 513 K) a volume premelted state is formed, manifesting itself in a growth of amplitudes of ion thermal vibrations, a steep increase of elementary cell volume and “softening” of lattice. The temperature dependence of order parameter for confined sodium nitrite was also determined. Order parameter follows a power law with $T_C = 425.6 \pm 2.1$ K, which is essentially different from that for bulk NaNO₂ [33,34].

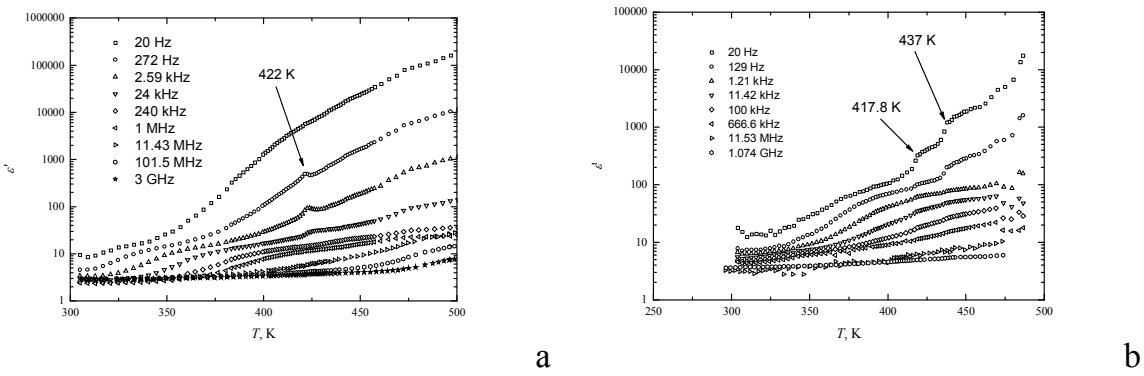


Figure 12. Temperature dependencies of the real part of dielectric permittivity of Sodium Nitrite confined in porous glass with 7nm (a) and 20 nm (b) pores.

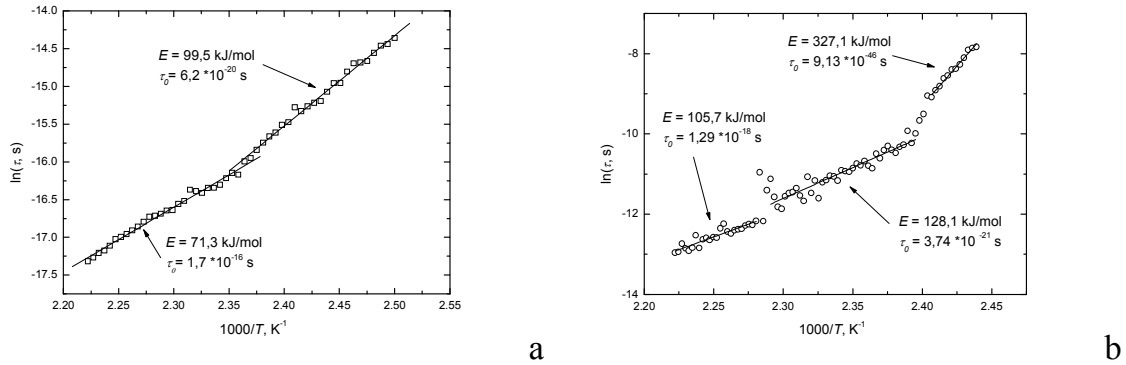


Figure 13. Temperature dependencies of obtained relaxation times of sodium nitrite confined in porous glass with 7nm (a) and 20 nm (b) pores.

Dielectric investigations of confined NaNO_2 in 7 nm pores showed that the phase transition is shifted to lower temperatures. Only one phase transition can be seen in the dielectric spectra and the intermediate incommensurate phase is suppressed (Figure 12a). The phase transition in nanoconfined NaNO_2 with pore size 20 nm remains nearly at the same temperature as in the bulk NaNO_2 . Two phase transitions can be seen in the dielectric spectra (Figure 12b): the first one exactly at 437 K and another one at 417 K., and it can be that incommensurate phase remains. The increase in the frequency dependent dielectric permittivity on heating is mainly the result of a conductivity effects. The relaxational soft mode contribution is as well present, but is small as compared to the conductivity contribution. Such huge conductivity is caused by a premelted phase, which is visible even at temperatures below the phase transition. Relaxational soft mode temperature behaviour is also different from classical ferroelectrics. Only change in the activation energy can be identified as phase transition (Figure 13). Present results confirmed value of T_C obtained from neutron scattering experiments. High level of conductivity most probably, can be caused by sodium. Similar conductivity is observed for NaNO_3 sample. Due to conductivity and premelted state relaxation time does not follow Arrhenius law in this material.

The main conclusions

- 1) Very broad distributions of relaxation times are characteristic for confined water and methanol molecules that are strongly interacting with the hosting matrix, which are caused by the formation of highly disordered hydrogen bonded network

at low temperatures ($T < 220$ K). Temperature evolution of most probable relaxation times depends on the pore size and chemical composition of the hosting matrix. No direct correlation between these parameters and relaxation peculiarities was found at higher temperatures.

- 2) Ferroelectric phase transition temperatures of betaine phosphite confined in MCM-41 molecular sieves are lower than those for bulk crystals. Confinement also changes the dynamics of betaine phosphite in the vicinity of the phase transition temperature.
- 3) No ferroelectric phase transitions were observed for barium titanate confined in MCM-41 molecular sieves. Permittivity maximums at 305 K and 315 K in dielectric responses are caused by adsorbed water and not by a ferroelectric phase transition (as suggested earlier).
- 4) Dielectric response of sodium nitrite confined in porous glasses is dominated by a giant increase of permittivity at low frequencies, which is caused by formation of a premelted phase. Relaxational soft mode temperature behaviour is also different from classical ferroelectrics. Only change in the activation energy can be identified as phase transition.

References

- [1] Wang X. S., Wang C. L., Zhong W. L., and Xue X. Y. *Ferroelectrics* **282** 49 (2003).
- [2] Radhakrishnan R., Gubbins K. E., Sliwinski-Bartkowiak M. *J. Chem. Phys.* **116** 56 (2002).
- [3] Beck J. S., Vartuli J. C., Roth W. J., Leonovicz M. E., Kresge C. T., Schmitt K. D., Chu C. T-W, Olson D. H., Sheppard E. W., McCullen S. B., Higgins J. B., and Shlenker J. L. *J. Am. Chem. Soc.*, **114** 10834 (1992).
- [4] Selvam P., Bhatia S. K., and Sonwane C. G. *Ind. Eng. Chem. Res.* **40** 3237 (2001).
- [5] Ying J. Y., Mehnert C. P. and Wong M. S. *Angew. Chem. Int. Ed. Engl.* **38** 56 (1999).
- [6] Sayari A., Danumah C. and Moudrakowski I. L. *Chem. Mater* **7** 813 (1995).
- [7] Ryoo R., Ko C. H., Kim J. M. and Howe R. *Catal. Lett.* **3** 29 (1996).
- [8] Chen L., Klar P. J., Heimbrod W., Brieler F. and Froba M. *Appl. Phys. Lett.* **76** 3531 (2000).
- [9] Leon R., Margolese D., Stucky G. and Petroff P. M. *Phys. Rev. B* **52** R2285 (1995).
- [10] Tang Y. S., Cai S., Jin G., Wang K. L., Soyey H. M. and Dunn B. S. *Appl. Phys. Lett.* **71** 2448 (1997).
- [11] Agger J. R., Anderson M. W., Pemble M. E., Terasaki O. and Nozue Y. *J. Phys. Chem. B* **102** 3345 (1998).
- [12] Kohiki S., Takad S., Shimizu A. and Yamada K. *J. Appl. Phys.* **87** 474 (2000).
- [13] Sliwinski-Bartkowiak M., Dudziak G., Sikorski R., Gras R., Radhakrishnan R. and Gubbins K. E. *J. Chem. Phys.* **114** 950 (2001).
- [14] Morishige K. and Ito M. *J. Chem. Phys.* **117** 8036 (2002).
- [15] Morishige K. and Kawano K. *J. Chem. Phys.* **110** 4867 (1999).

- [16] Hansen E. W., Stocker M. and Schmidt R. *J. Phys. Chem.* **100** 2195 (1996).
- [17] Kremer F., Huwe A., Schonhals A. and Rozanski S. A. *Broad Band Dielectric Spectroscopy* ed Kremer and Schonhals (Berlin: Springer) p 171 (2003).
- [18] Wu C.-G. and Bein T. *Chem. Mater.* **6** 1109 (1994).
- [19] Warnock J., Awshalom D. D., Shafer M. W. *Phys. Rev. Lett.* **57** 1753 (1986).
- [20] Overloop K., Gerven L. V. *J. Magn. Reson.* **101** 179 (1993).
- [21] Macutkevic J., Banys J., Matulis A. *Nonlinear Analysis: Modelling and Control* **9- 1** 75 (2004).
- [22] Ryabov Ya., Gutina A., Arkhipov V. and Feldman Yu. *J Phys. Chem. B* **105** 1845 (2001).
- [23] Yamaguchi T., Hidaka K. and Soper A. K. *Mol. Phys.* **96** 1159 (1999).
- [24] Adya A. K., Bianchi L. and Wormald C. J. *J. Chem. Phys.* **112** 4231 (2000).
- [25] Narten A. H. and Habenschuss A. *J. Chem. Phys.* **77** 2051 (1982).
- [26] Jorgensen W. *J. Phys. Chem.* **90** 1276 (1986).
- [27] Kosztolanyi T., Bako I., and Palinkas G. *J. Chem. Phys.* **118** 4546 (2003).
- [28] Morishige K. and Kawano K. *J. Chem. Phys.* **112** 11023 (2000).
- [29] Guegan R., Morineau D., Alba-Simionesco C. *Chemical Physics* **317** 236 (2005).
- [30] Fehst I., Paasch M., Hutton S. L., Braune M., Bohmer R., Loidl A., Dorfel M., Narz Th., Haussuhl S. and McIntyre G. J. *Ferroelectrics* **138** 1 (1993).
- [31] Albers J. *Ferroelectrics* **78** 3 (1988).
- [32] Bierwirth E. “NMR studies on ferroelectrics in confined geometry” diploma thesis Institute of Experimental Physics II Leipzig May 28 (2004).
- [33] Fokin A.V., Kumzerov Yu. A., Okuneva N.M., Naberezhnov A. A. and Vakhrushev S. B. *Physical Review Letters* **89** 17 (2006).
- [34] Naberezhnov A., Fokin A., Kumzerov Yu., Sotnikov A., Vakhrushev S., and Dorner B. *Eur. Phys. J. E*, **12** s01 006. (2003).

Short CV of the author

1998-2002 Telecommunication physics and electronics studies, Vilnius university, Faculty of Physics. Graduated 2002.

2002-2004 M.Sc. studies, Vilnius University, Faculty of Physics. Graduated 2004.

2004-2008 Ph.D. student, Vilnius University, Faculty of Physics.

List of publications

- 1) J. Banys, M. Kinka, J. Macutkevic, G. Volkel, W. Bohlman, V. Umamaheswari, M. Hartmann, and A. Poppl *J. Phys.: Condens. Matter*, **17** (2005) 2843-2857
“Broadband Dielectric Spectroscopy Of Water Confined In MCM-41 Molecular Sieve Materials – Low-Temperature Freezing Phenomena”
- 2) J. Banys, M. Kinka, A. Meskauskas, J. Macutkevic, G. Volkel, W. Bohlman, V. Umamaheswari, M. Hartmann and A. Poppl *Ferroelectrics*, **318** (2005) 201–207

- “Broadband Dielectric Spectroscopy Of Water Confined In MCM -41 Molecular Sieve Material”
- 3) M. Kinka, J. Banys, W. Böhlmann, E. Bierwirth, M. Hartmann, D. Michel, G. Völkel and A. Pöpl *J. Phys. IV France*, 128 (2005) 81-85 “Dielectric Spectroscopy Of BaTiO₃ Confined In MCM -41 Mesoporous Molecular Sieve Materials”
 - 4) M. Kinka, J. Banys, J. Macutkevic, A. Pöpl, W. Böhlmann, V. Umamaheswari, M. Hartmann and G. Völkel *Phys. Stat. Sol. (B)*, 242, No. 12, (2005) R100–R102 / Doi 10.1002/Pssb.200541038 www.pss-rapid.com “Dielectric Response Of Water Confined In MCM -41 Molecular Sieve Material”
 - 5) J. Banys, M. Kinka, J. Macutkevic, G. Völkel, W. Böhlmann, V. Umamaheswari, M. Hartmann and A. Pöpl *Materials Science Forum*, Vols. 514-516 (2006) 1255-1259 “Effect Of Confinement On The Freezing-melting Dynamics Of Water”
 - 6) M. Kinka, J. Banys, J. Macutkevic and A. Meskauskas *Electrochimica Acta*, 51 (2006) 6203–6206 “Conductivity Of Nanostructured Mesoporous Mcm-41 Molecular Sieve Materials”
 - 7) M. Kinka, J. Banys, W. Bohlmann, E. Bierwirth, M. Hartmann, D. Michel, G. Volkel and A. Poepl *IEEE Transactions on Ultrasonics, Ferroelectrics, and Frequency Control*, 53 (2006) 2305-2308. DOI: 10.1109/TUFFC.2006.178 “Dielectric Spectroscopy of Nano BaTiO₃ Confined in MCM-41 Mesoporous Molecular Sieve Materials”
 - 8) J. Banys, M. Kinka, G. Volkel, W. Bohlman, V. Umamaheswari, M. Hartmann and A. Poppl *Ferroelectrics*, 353 (2007) 97 – 103. DOI: 10.1080/00150190701368042 “Dielectric Spectroscopy of Betaine Phosphite confined in MCM-41 Molecular Sieve Materials”
 - 9) M. Kinka, J. Banys and A. Naberezhnov *Ferroelectrics*, 348 (2007) 67-74. “Dielectric Properties of Sodium Nitrite Confined in Porous Glass”
 - 10) M. Kinka, J. Banys, G. Volkel, W. Bohlman, V. Umamaheswari, M. Hartmann, and A. Poppl, *Наносистеми, наноматеріали, нанотехнології Nanosystems, Nanomaterials, Nanotechnologies*, т. 5, № 2 (2007) сс. 631–639 “Dielectric

Spectroscopy of Mesoporous MCM-41 Molecular Sieve Materials Containing Betaine Phosphite”

- 11) J. Banys, M. Kinka, A. Meskauskas, R. Sobiestianskas, G. Volkel, W. Bohlmann, M. Hartmann and A. Poppl *Ferroelectrics*, 346 (2007) 173–180. “Effect Of Confinement On The Dynamics Of Methanol”
- 12) J. Banys, M. Kinka, G. Völkel, W. Böhlmann, A. Pöppl *Appl. Phys. A* [10.1007/S00339-008-5052-7](https://doi.org/10.1007/S00339-008-5052-7), 2009 “Dielectric Response Of Water Confined In Metal–Organic frameworks”

Reziume

Šiame darbe pateikiami vandens, metanolio ir įvairių feroelektrikų, apribotų porėtose medžiagose, dielektrinės dinamikos tyrimų plačiuose dažnių ir temperatūrų intervaluose dielektrinės spektroskopijos metodu rezultatai. Įvade supažindinama su šių tyrimų aktualumu ir praktine svarba, formuluojami darbo uždaviniai, ginamieji teiginiai bei pateikiamas gautų rezultatų mokslinis naujumas, disertacijos tema paskelbtų straipsnių prestižiniuose mokslo žurnaluose bei pranešimų konferencijose sąrašai. Antrajame skyriuje apžvelgiami Lietuvoje ir užsienyje atlikti porėtose matricose apribotų medžiagų tyrimai. Pirmajame poskyryje aprašoma porėtų medžiagų klasifikacija, pateikiama informacija apie medžiagų, kurios buvo naudojamos šiame darbe kaip laikančiosios matricos apriboto vandens, metanolio bei feroelektrikų dinamikos tyrimams, sandarą, fizikines savybes ir sintezės būdus. Antrajame poskyryje aptariama žinoma apribojimo įtaka adsorbuotų skysčių savybėms, lydimosi bei kristalizacijos dinamikai. Trečiajame – matmenų mažėjimo ir sąveikos su laikančiąja matrica įtaka apribotų medžiagų feroelektrinėms savybėms. Trečiajame skyriuje aprašyti tyrimams naudoti dielektrinės spektroskopijos metodai ir matavimo priemonės, jų taikymo ribos ir apribojimai. Ketvirtajame skyriuje pateikiami gauti dielektrinių tyrimų rezultatai, bei analizuojamas jų santykis su kitų tyrėjų duomenis. Šis skyrius suskirstytas į penkis poskyrius, kiekviename kurių aprašomos skirtingų apribotų medžiagų savybės. Juose paeiliui aprašomi vandens molekulių, apribotų MCM-41, AlMCM-41, CPG ir MOF medžiagose, metanolio molekulių, apribotų MCM-41 bei AlMCM-41 medžiagose, betaino fosfito, apriboto trijuose skirtingo porų dydžio (2,0 nm, 2,5 nm ir 3,7 nm) MCM-41 sietuose, MCM-41 molekulinuose sietuose susintetinto bario titanato bei natrio nitrito, apriboto porėtuose stikluose su 7 nm ir 20 nm dydžio poromis, dielektrinės skvarbos tyrimų rezultatai. Analizuojami lydimosi – užšalimo bei feroelektrinių fazinių virsmų dinamikos ypatumai, laikančiosios medžiagos cheminės sandaros, porų išsidėstymo bei jų dydžio įtaka. Darbo gale pateikiamos svarbiausios išvados ir naudotos literatūros sąrašas.